Available online at www.sciencedirect.com
SCIENCE DIRECT®
Journal of Photochemistry and Photobiology A: Chemistry 159 (2003) 289–300
Journal of Photochemistry and Photobiology A:Chemistry
www.elsevier.com/locate/jphotochem

Environmental remediation by an integrated microwave/UV-illumination technique IV. Non-thermal effects in the microwave-assisted degradation of 2,4-dichlorophenoxyacetic acid in UV-irradiated TiO_2/H_2O dispersions

Satoshi Horikoshi [a], Hisao Hidaka [a,*], Nick Serpone [b]

[a] *Frontier Research Center for the Global Environment Protection (EPFC), Meisei University, 2-1-1 Hodokubo, Hino, Tokyo 19l-8506, Japan*
[b] *Department of Chemistry and Biochemistry, Concordia University, 1455 de Maisonneuve Boulevard West, Montreal, Que., Canada H3G 1M8*

Received 21 November 2002; received in revised form 22 February 2003; accepted 15 March 2003

Abstract

After establishing proof of concept in the first three articles of this series, in which we used the rhodamine-B dye to test the methodology, we herein report a study on the photocatalyzed degradation of 2,4-dichlorophenoxyacetic acid (2,4-D) in aqueous TiO_2 dispersions that were subjected to simultaneous irradiation by UV light and microwave (MW) radiation. The characteristics of the process were monitored for the effect of microwave radiation by examining the fate of each substituent group, viz. the carboxylic acid group, the chlorine substituents and the benzene ring of the 2,4-D structure. The degradation dynamics of the microwave-assisted process were examined by decrease of UV absorption, loss of total organic carbon (TOC), formation of Cl^- ions (dechlorination), and identification of intermediates by electrospray mass spectral techniques. The thermal effect of the microwave radiation to the system was considered by comparing results from MW-generated heat versus externally applied heat. The effect of dissolved oxygen or absence of oxygen on the degradative process was also investigated. The greater efficiency of the MW-assisted process is ascribed to a non-thermal effect of microwave radiation on the break-up of the aromatic ring of 2,4-D (oxidation) but evidently not on the dechlorination process (reduction) for which MW radiation seems to have a negligible influence, if any. Factors involved in this non-thermal component and a mechanism are proposed for the initial stages of the degradation.

Keywords: Photooxidation; Photodegradation; Microwave radiation; 2,4-Dichlorophenoxyacetic acid; Titanium dioxide; Photocatalysis; Agricultural chemicals

1. Introduction

The agricultural chemical 2,4-dichlorophenoxyacetic acid (2,4-D) is a typical widely used and highly toxic synthetic phytohormone (toxin). Not surprisingly, the United States Environmental Protection Agency has classified 2,4-D as a suspected endocrine disruptor. Many studies have been reported on the photocatalyzed decomposition of chlorinated toxic compounds such as the agrochemicals containing the triazine skeleton (Atrazine) [1–4], 2,4-D [5–8], dibromochloropropane [9–11], hexachlorocyclohexane [11], *p,p′*-DDT [12,13], *p,p′*-DDE [14], 2,4-dichlorophenol [15–19], kelthane [20], polychlorinated biphenyls (PCB) [21–24], polychlorinated dibenzo-*p*-dioxins [22,25,26], pentachlorophenol (PCP) [27–31], and 2,4,5-trichlorophenoxyacetic acid [32]. Complete dechlorination (reduction reaction) of many chlorinated compounds by the photocatalytic degradative route tends to be rather slow toward the mineralization of organic carbon atoms (oxidation reaction) to carbon dioxide. Dechlorination of chlorinated systems is improved greatly when using platinized TiO_2 aqueous dispersions [33], albeit the photocatalytic process occurring in these TiO_2/Pt dispersions can be rather expensive. Accordingly, treatment of large quantities of chlorinated pollutants is not likely to be economically viable. Alternatives are thus desirable. We have recently reported that the cationic rhodamine-B dye, a typically difficult dye to degrade, can be decomposed efficiently by concomitant

* Corresponding author. Tel.: +81-44-591-6635; fax: +81-44-599-7785.
E-mail addresses: hidaka@epfc.meisei-u.ac.jp (H. Hidaka), serpone@vax2.concordia.ca (N. Serpone).

1010-6030/03/$ – see front matter © 2003 Elsevier Science B.V. All rights reserved.
doi:10.1016/S1010-6030(03)00185-0

irradiation of dye/TiO_2 suspensions with UV light and microwave radiation [34–38]. The latter studies established proof of concept of the methodology.

In this study, we examine the degradation of an aqueous solution of 2,4-D in the presence of TiO_2 particles irradiated concomitantly by microwaves and UV light. The strategy of our study was fourfold: (i) assess the generality of the coupled MW/photocatalytic routes by examining the photodegradation of 2,4-D under concomitant illumination with microwave radiation and UV light; (ii) assess the different pathway characteristics of the degradation of 2,4-D illuminated by UV light alone and by integrated UV/MW radiation; (iii) assess the degradative features of photooxidation and photoreduction under air-equilibrated conditions, as well as in oxygen- and nitrogen-purged dispersions; (iv) examine the degradation of 2,4-D using a microwave-powered double quartz cylindrical plasma photoreactor (DQCPP), and finally assess what factors of the microwave radiation influence the photomineralization process.

2. Experimental

2.1. Chemical reagents and degradation procedures

The photocatalyst was Degussa P-25 TiO_2 (BET specific surface area, 53 $m^2\,g^{-1}$; particle size, 20–30 nm by TEM; composition, 83% anatase, 17% rutile by X-ray diffraction). High purity grade 2,4-dichlorophenoxyacetic acid (2,4-D) was supplied by Wako Pure Chem. Co.

Microwave irradiation was carried out with a Shikoku Keisoku ZMW-003 system (Fig. 1) manufactured by Shibaura Mechatronics Co. Ltd. It consisted of a microwave generator (frequency, 2.45 GHz; maximal power, 1.5 kW), a three-stub tuner, a power monitor, and an isolator. Microwave radiation (single-mode operation; actual power used, 300 W) used to irradiate the 2,4-D air-equilibrated aqueous solution (0.1 mM, 30 ml) containing TiO_2 particles (loading, 60 mg) was delivered through a wave-guide. Optimal low reflection of the MW radiation was achieved using the three-stub tuner. The UV irradiation source was an Ushio 250 W mercury lamp, whose UV radiation was fed to the 250 ml Pyrex cylindrical reactor ($\phi = 45 \times 290$ mm; Taiatsu Techno® Co.; maximum pressure, 1 MPa; maximum temperature, 150 °C) by a fiber optic light-guide. The dispersion was continually stirred during irradiation. The reactor was sealed with two Teflon rings and a stainless steel cap. The gas phase in the headspace volume of the reactor contained air, O_2 or N_2 gases. Introduction of O_2 and N_2 into the cylindrical photoreactor was achieved by reducing the pressure by 0.1 MPa with a diffusion pump, after which a 0.1 MPa quantity of O_2 or N_2 gas was introduced into the closed reactor. The procedure was repeated for no less than five times. The UV source and the microwave generator were located on the front side and right side of the device, respectively. Both radiation sources were set at 90° to each other (inset in Fig. 1).

2.2. Experimental technique

The decomposition of 2,4-D was achieved by four different routes. (i) Photocatalytic degradation under UV light and microwave irradiation of air-equilibrated, O_2- or N_2-purged 2,4-D/TiO_2 dispersions; the routes taken are referred to as PD/MW, PD/MW_{O_2} and PD/MW_{N_2}. The temporal profile of temperature in the aqueous 2,4-D/TiO_2 dispersion is shown in the inset in Fig. 1. The maximal temperature was 137 °C. (ii) Photocatalytic degradation of 2,4-D/TiO_2 dispersions by UV irradiation alone under otherwise similar gaseous conditions, viz. PD, PD_{O_2} and PD_{N_2}. (iii) Microwave irradiation of the 2,4-D solution in the absence of the TiO_2 catalyst (MW). (iv) Photocatalytic degradation of the 2,4-D/TiO_2 dispersions with UV light and externally applied heat (PD/TH). For the latter purpose, one part of the cylindrical photoreactor used was coated with a metallic film using the MOCVD technique on one side at the bottom of the reactor; the applied voltage was 100 V or less. The other side of the reactor was not coated so that UV irradiation could be used to photodecompose the 2,4-D herbicide. Temperature (error less than 1 °C) and pressure were controlled in a manner identical to that used for the PD/MW method. The degradation by the MW and PD/TH routes was performed only under air-equilibrated conditions.

2.3. Photocatalytic degradation of 2,4-D using the DQCPP lamp

The double quartz cylindrical plasma photoreactor (DQCPP) (dimensions: 10 cm (length) × 7 cm (external diameter) × 1 cm (internal diameter)) contained mercury gas and a very small quantity of argon gas introduced as a purge gas in the DQCPP lamp device after bringing the system to vacuum (ca. 10^{-3} Pa). The quartz pipe photoreactor was placed in the center of the DQCPP device. It was connected to a Teflon tube (2 m long and $\phi = 9$ mm) through which the 2,4-D aqueous solution containing TiO_2 particles was circulated employing a peristaltic pump (150 ml; flow rate, 2000 ml min^{-1}; 2,4-D concentration, 0.1 mM; TiO_2 loading, 170 mg). When using the DQCPP device, the system was changed from single-mode operation to a multi-mode operation in a stainless steel microwave oven (internal dimensions: 47 cm (width) × 50 cm (height) × 56 cm (depth)). The microwave power was ca. 330 W (continuous). The temperature of the solution was maintained at 27 ± 1 °C with a cooling circulator device (Fig. 2).

The PD/MW methodology for the degradation of the 2,4-D substrate was examined with the DQCPP device using both a conventional Hg lamp and an electrodeless Hg lamp powered by microwave radiation. The two UV electrode Hg lamps (dimensions: 10 cm (length) × 3 cm (diameter); Toshiba 75 W) were located on top and bottom of the quartz

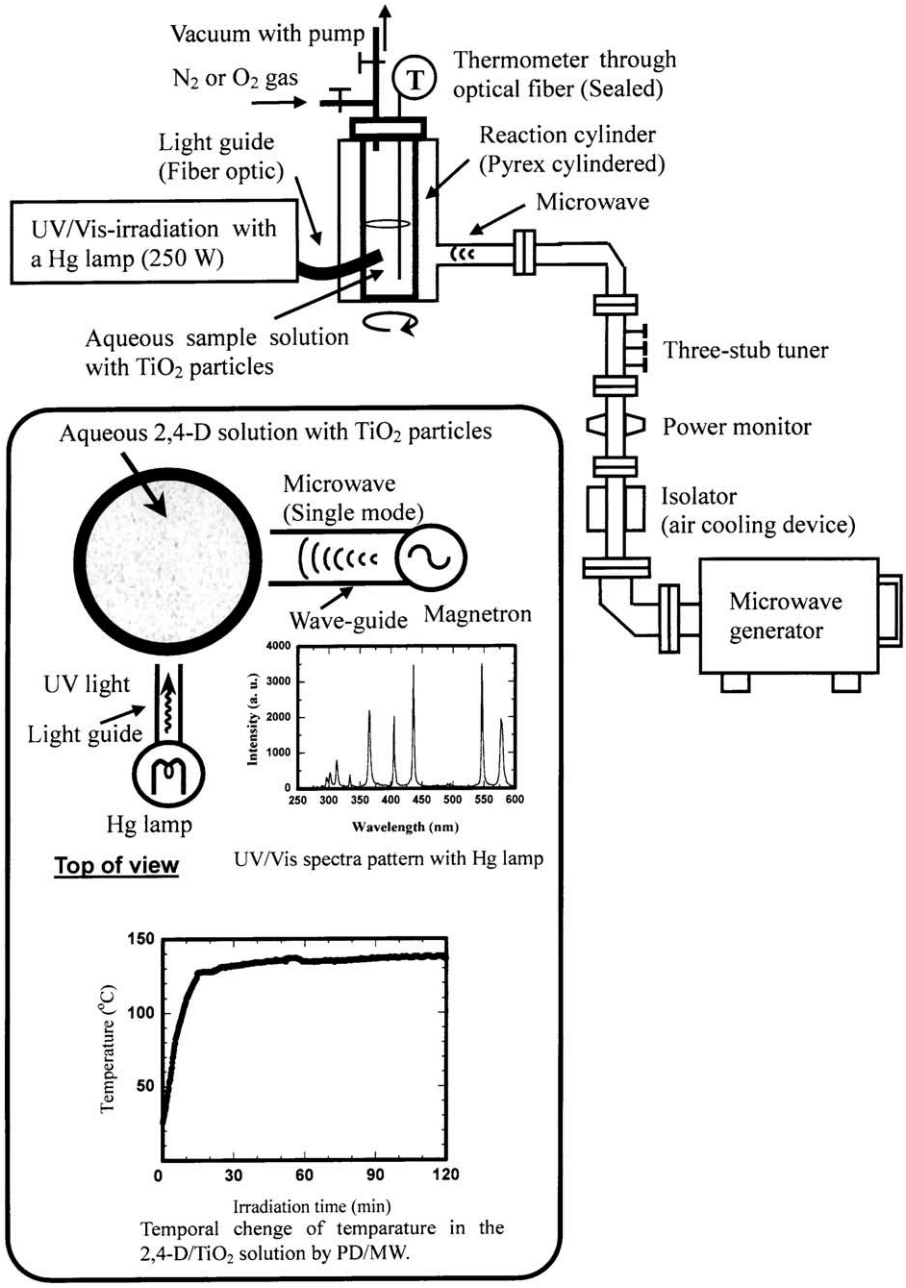

Fig. 1. Experimental set-up for the UV and microwave irradiation system used to irradiate the dispersions.

pipe (see inset in Fig. 2). A two-electrode Hg lamp system was used in the PD method; two quartz cylindrical plasma lamps (QCPL; dimensions: 10 cm (length) × 3 cm (diameter)) containing Hg gas were also used for the PD method when using two electrode mercury lamps. The internal Hg gas in the QCPL lamps was the same as for the DQCPP device, and their location in the microwave oven was identical to the positions of the 75 W Hg lamps (total power, 150 W; see second inset in Fig. 2). The power of the electrodeless Hg lamps (QCPL) was also 150 W. The Hg lamps and the QCPL lamps emitted an irradiance of 12 mW cm^{-2} and ca. 4 mW cm^{-2} per lamp, respectively, in the wavelength range 310–400 nm (maximal emission at $\lambda = 360$ nm). The temperature of the aqueous 2,4-D solution was also maintained constant at $27 \pm 1\,^{\circ}$C (see above).

2.4. Analytical procedures

The temporal disappearance of the UV absorption features and changes in total organic carbon (TOC) during the degradation of 2,4-D were monitored with a JASCO UV-Vis/NIR V-560V spectrophotometer and a Shimadzu TOC-5000A analyzer, respectively. Formation of carboxylic acid intermediates was determined using a JASCO HPLC system in

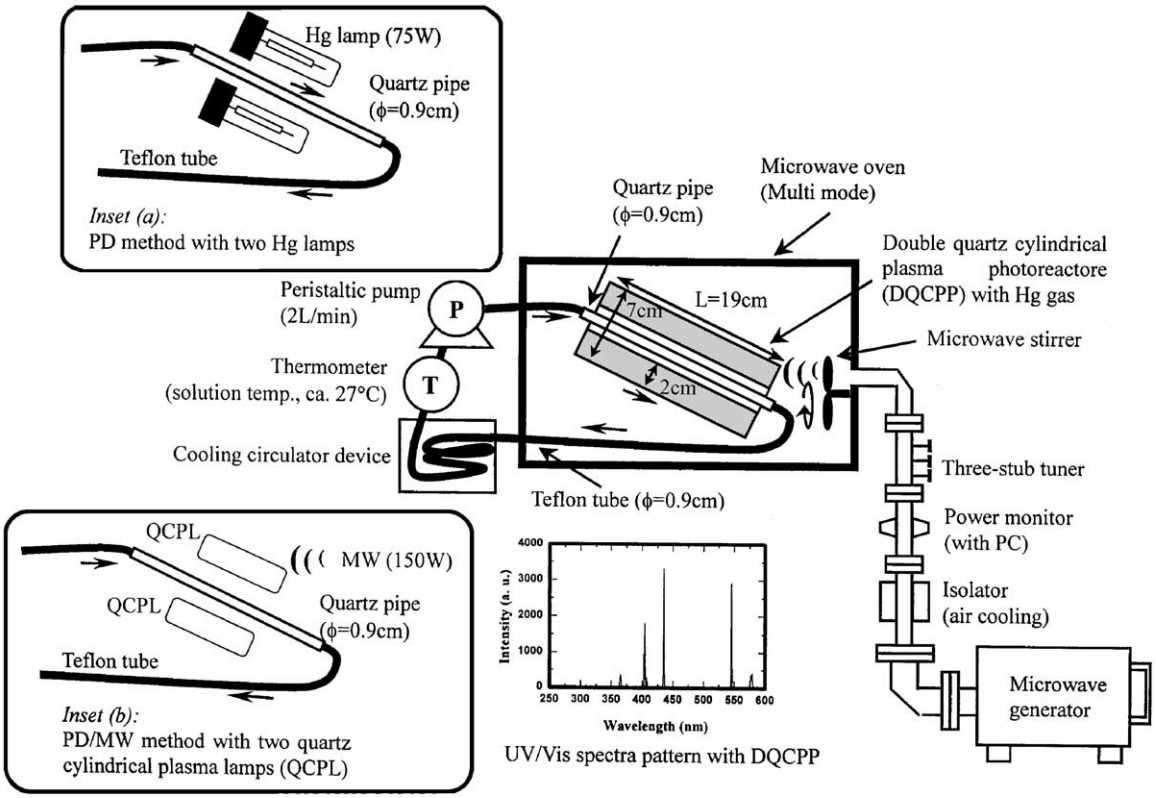

Fig. 2. Experimental set-up of the double quartz cylindrical photoreactor (DQCPP) used in the photocatalytic decomposition of 2,4-D in aqueous TiO_2 dispersions using integrated UV and microwave radiations used to irradiate the dispersions.

the presence of bromthymol blue as an indicator. The intermediates produced from the degradation of the 2,4-D were identified using an Agilent Technologies HP1100 series LC–MSD (liquid chromatograph coupled to an electrospray mass spectral detector operated in the negative and positive modes) apparatus; the eluent was a mixed solution of methanol and water (1:1 v/v), and the column was an Agilent Eclipse XDB-C_8 column. The mass spectra from the API-ES ionization mode were recorded under conditions where the fragmenter was set at 100 V, the capillary voltage was 2800 V and the dry gas temperature was 300 °C.

The UV absorption spectral features of 2,4-D were simulated using the ZINDO software version 6.3 in the Fujitsu CAChe package implemented on a Pentium IV computer. The UV-Vis electronic transitions were calculated with the ZINDO program using INDO/1 parameters after optimizing the geometry with Augmented MM3 and PM3 in the MOPAC software [39].

3. Results and discussion

An aqueous solution of 2,4-dichlorophenoxyacetic acid displays absorption bands at 285, 230 and 204 nm. Calculations of absorption band positions with the ZINDO software for the chemical structure of 2,4-D indicated that the 230 and 285 nm bands are likely those of a substituted benzene ring containing two chlorines and one carboxylic acid group, whereas the 204 nm band is consistent with absorption by a naked benzene ring. Loss of UV absorption features at these three wavelengths and loss of total organic carbon, together with formation of Cl^- ions subsequent to dechlorination and decomposition of air-equilibrated 2,4-D aqueous solutions by the MW, PD, PD/TH and PD/MW routes are reported in Fig. 3. It is evident that microwave irradiation alone of the aqueous dispersion had no effect whatever on the break-up of the aromatic ring of 2,4-D (i.e. loss of UV absorptions), on the loss of TOC, and on the dechlorination of the 2,4-D toxin.

Initially (<15 min), differences in UV absorption loss for the PD and PD/TH routes were, within experimental error, negligibly small for the other three methods. However, further irradiation showed significant variations, with the order of decrease of the quantity of 2,4-D assayed by loss of absorption spectral features at the three wavelengths being PD/MW > PD/TH > PD after 60 min of irradiation. The photocatalytic PD route was the slowest process of the three (Fig. 3a–c). Moreover, at all three wavelengths the PD/TH process was slower than the PD/MW process, even though the temperature of the dispersion from the heat generated by the MW radiation and from heat externally applied was identical in both cases. The same was also observed for TOC decay and for the dechlorination of the 2,4-D toxin. Curiously, however, the dynamics of dechlorination by the PD

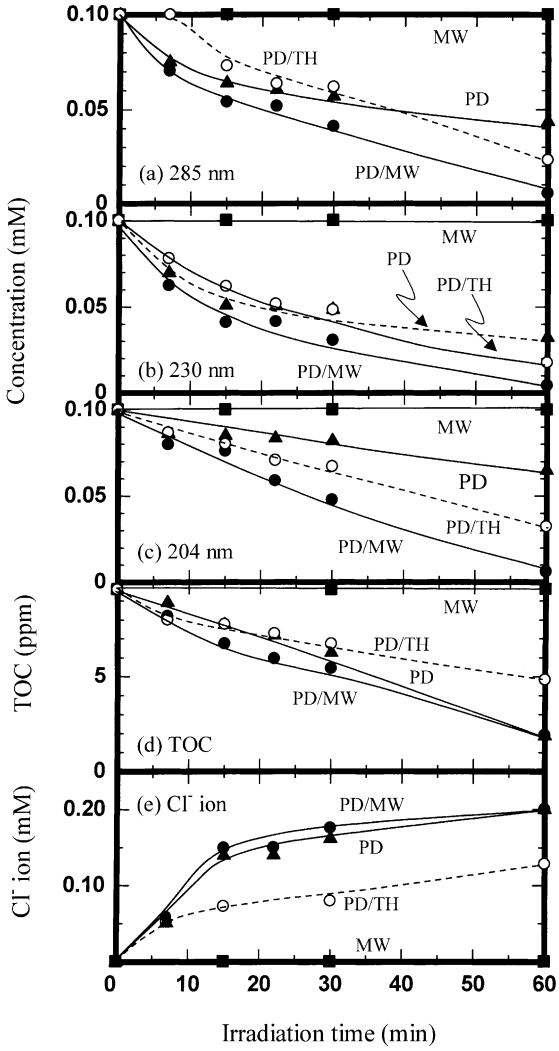

Fig. 3. Decrease of UV absorption and total organic carbon (TOC), together with formation of Cl^- ions in the decomposition of 2,4-D (0.10 mM) in aqueous media by microwave irradiation (MW), photocatalyzed oxidation (PD), thermally-assisted photocatalyzed oxidation (PD/TH) and integrated microwave-assisted photocatalyzed degradation (PD/MW) under air-equilibrated conditions.

route were the same as for the PD/MW route in the formation of chloride ions. Evidently, the MW radiation was silent on the dechlorination events, which is understandable if dechlorination occurred mostly through a reductive path involving photogenerated electrons.

We infer that microwave radiation acts predominantly on the oxidative route to degradation of the substrate, and appears to have relatively little impact on the reductive events occurring at the TiO_2 particle surface. In addition, the factors that influence the faster dynamics of the oxidative degradation of 2,4-D by the PD/MW relative to those by the PD/TH route are likely related to non-thermal effects caused by the MW radiation [40]. Note, however, that both thermal and non-thermal effects are operative on the oxidative degradation of 2,4-D; compare, for example, the PD route with the PD/TH and PD/MW pathways. Extensive studies [41] on microwave-assisted photochemical syntheses of various organic compounds in homogeneous media have proposed that the faster dynamics in these cases originate with an athermal (i.e. non-thermal) effect from the microwaves, which was attributed to changes in the pre-exponential factor A in the Arrhenius equation, $k = Ae^{-Ea/RT}$. In the present instance, however, we cannot preclude specific interactions of the microwave radiation with the UV-illuminated TiO_2 particle surface. Such interactions may give rise to the generation of additional surface defects [42] that can directly increase the concentration of $^{\bullet}OH$ radicals [43] or some other but equivalent reactive oxygen species in the aqueous dispersion. In accord with this notion, a recent model proposed by Booske et al. [44] to explain non-thermal effects suggests that microwave radiation can couple into the low (MW) frequency elastic lattice oscillations of a crystalline solid, thereby generating a non-thermal distribution that might enhance ion mobility and thus diffusion of charge carriers (in our case) to the surface leading to increased formation of surface $^{\bullet}OH$ radicals and to increased concentration of electrons at the surface. Note that the relative concentration of the two charge carriers (electrons and holes) at the surface is a very sensitive function of the surface potential [45]. The model also infers resonant coupling of microwave photons to weak bond surface modes and to point defect modes, as well as non-resonant coupling to zero-frequency displacement modes. Clearly, the surface of the TiO_2 particles is significantly perturbed by the microwave radiation with the net result, as observed experimentally, that the photodegradation of pollutant organic substrates will become more efficient under coupled UV/MW irradiation relative to UV irradiation alone.

One of the important factors for the efficient photodegradation of organic pollutants using TiO_2 photocatalysis is dependent on the concentration of $^{\bullet}OH$ radicals formed by the photooxidation of surface OH^- ions and/or H_2O in aqueous media in the absence of the 2,4-D substrate. A flow-type cylinder was employed for this experiment (see Fig. 4a). The number of $^{\bullet}OH$ radicals formed was determined in water alone (250 ml) under MW irradiation (350 W) alone, by the PD route in an UV-irradiated aqueous TiO_2 dispersion (loading, 250 mg), and by the integrated PD/MW route for a UV irradiation period of 1 min. To the extent that the 5,5-dimethyl-1-pyrrolidine-*N*-oxide (DMPO) spin-trapping behavior was rather complex at the higher temperatures, experiments were conducted with the temperature of water fixed at 26 °C by employing a cooling jacket. The solution was circulated at 2 l min^{-1} with a pump. The ESR spectral peak intensity was automatically calculated relative to the Mn^{2+} standard marker inside the ESR cavity (JEOL JES-TE200 ESR spectrometer). The ESR spectral patterns for each degradation route in aqueous TiO_2 dispersions without the substrate are compared in Fig. 4b. The 1:2:2:1 spectral signature of the DMPO–$^{\bullet}OH$ spin adduct for evidence of formation of $^{\bullet}OH$ radicals is unmistakable.

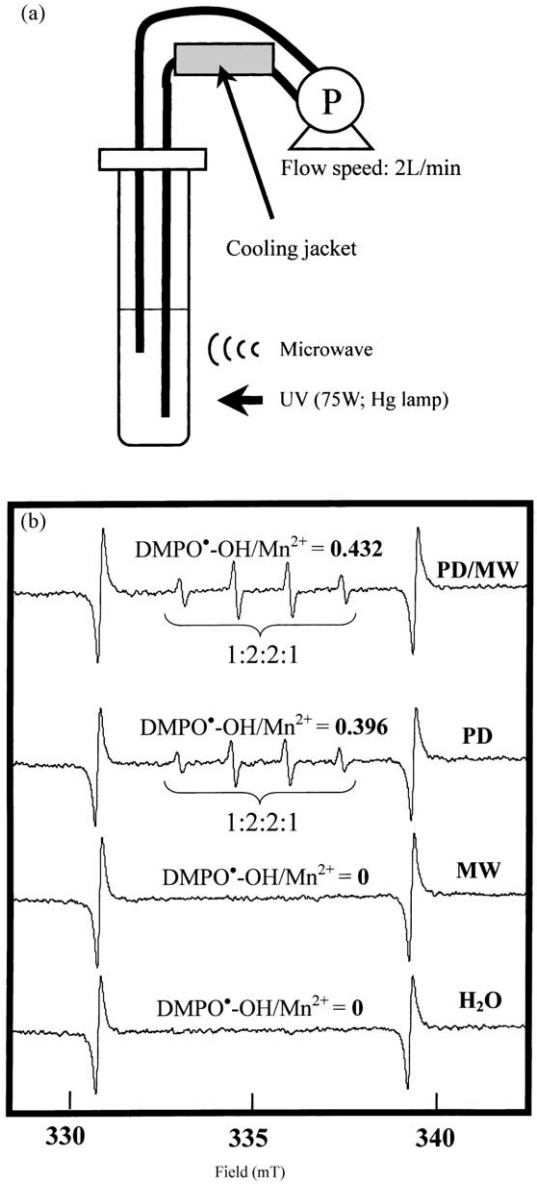

Fig. 4. (a) Set-up used to generate •OH radicals in water alone under MW irradiation, in an aqueous TiO_2 dispersion by the PD route, and by the integrated PD-MW route. The input power of the MW radiation was 350 W; the UV irradiation source was a 75 W mercury lamp. A peristaltic pump was used to circulate the aqueous TiO_2 dispersion at a flow rate of 2 l min^{-1}. The temperature of the system was maintained at ca. 26 °C using a water-cooling device located outside the MW apparatus. (b) Spectral patterns for the DMPO–•OH spin adduct under the conditions indicated (see text for further details). The relative quantity of •OH radicals formed was estimated automatically against an internal Mn^{2+} standard marker.

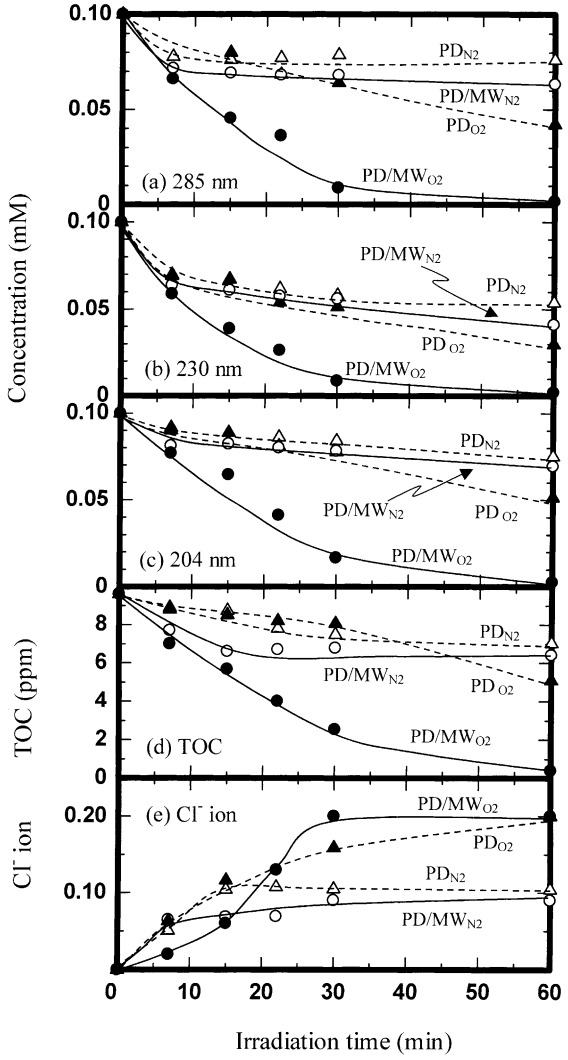

Fig. 5. Disappearance of UV absorption and TOC, along with formation of Cl^- ions in the degradation of 2,4-D by the PD and PD/MW methods in oxygenated and partially deoxygenated media.

Clearly, formation of •OH radicals by the PD/MW route was more efficient than that by the PD route.

Fig. 5 reports and compares the results of the degradative process for 2,4-D monitored also by the loss of UV absorption at 285, 230 and 204 nm, loss of TOC, and dechlorination using the PD and PD/MW routes for oxygen- and nitrogen-purged 2,4-D/TiO_2 dispersions. The most significant difference seen in the loss of UV absorption features in the first 30 min of irradiation was the relatively fast degradation of the 2,4-D structure by the PD/MW_{O_2} route, compared to the PD_{N_2}, PD_{O_2} and PD/MW_{N_2} routes; the latter showed similar dynamics at least in the first 30 min of irradiation (see Fig. 5a–c). After 60 min of irradiation, the PD/MW_{O_2} route led to total loss of UV absorptions at all three wavelengths, indicating quantitative degradation of the 2,4-D toxin. The order of efficiency of the four routes was: $PD/MW_{O_2} >>> PD_{O_2} > PD/MW_{N_2} > PD_{N_2}$.

Loss of TOC in Fig. 5d is consistent with the UV spectral observations (Fig. 5a–c), and the relative order of efficiency is identical to the one above. Nearly complete decay of TOC in the 2,4-D/TiO_2 dispersion was seen after 60 min of irradiation by the PD/MW_{O_2} route. Significant variations were seen in the first 30 min in the formation of chloride ions for all four routes examined (see Fig. 5e). After 60 min, however, dechlorination was complete by the PD/MW_{O_2}

and PD_{O_2} routes producing 0.20 mM of chloride ions, as expected. By contrast the quantity of Cl^- ions, produced by the PD/MW_{N_2} and PD_{N_2} routes in nitrogen-purged dispersions, was only ca. 0.10 mM reflecting loss of only one chlorine substituent from the 2,4-D ring. As alluded to earlier, the latter event was probably caused either by a slower photoreductive process and/or by the near-absence of oxygen (see below) in the dispersion.

The quantity of dissolved oxygen in the 2,4-D solution subjected to the PD/MW_{N_2} and PD_{O_2} routes was measured with a Horiba D-25 detector prior to and after 30 min irradiation. In the PD/MW_{N_2} case, the amount of dissolved oxygen was initially 2.4 mg l^{-1} dropping to 1.4 mg l^{-1} after 30 min. By contrast, the initial quantity of dissolved oxygen in the PD_{O_2} route was 9.8 mg l^{-1}, dropping only slightly to 9.7 mg l^{-1} after 30 min. The significant differences seen between the PD/MW_{O_2} and PD/MW_{N_2} for the extent of degradation of 2,4-D, loss of TOC, and the degree of dechlorination are noteworthy. Similar variations were not observed when comparing the PD_{O_2} and PD_{N_2} routes. Evidently, microwave irradiation has some direct or indirect effect on the overall degradation of 2,4-D in oxygenated and nitrogen-purged solutions. This inference is consistent with the notion that MW radiation can cause additional surface defects on the TiO_2 particle surface and involves oxygen. It cannot be a simple and sole direct effect on the pre-exponential factor (see above).

On the basis of the above results and discussion, we deduce that dechlorination occurring during the decomposition of 2,4-D likely takes place through two differing pathways depending on whether the solution is initially oxygen-saturated or is partially deoxygenated. TiO_2 particles absorb UV light of energy greater than the bandgap (ca. 3.2 eV) to generate electron/hole pairs (Eq. (a)), followed by various steps in which the holes (h^+) are ultimately trapped by OH^- ions (or by H_2O) at the particle surface to yield $^\bullet OH$ radicals (and H^+; Eq. (b)), which are the major oxidizing radicals in the oxidative degradation of 2,4-D. Concomitantly, in oxygen-purged dispersions the dioxygen molecules react with the conduction band electrons (e^-; Eq. (c-1)) in competition with the 2,4-D substrate (Eq. (c-2)) to yield the superoxide radical anions, $O_2{}^{-\bullet}$, which on protonation generate the hydroperoxy radicals ($^\bullet OOH$; Eq. (c-3)). By contrast, in nitrogen-purged dispersions, direct attack of the 2,4-D substrate by the electrons is more pronounced (Eq. (d) versus Eq. (c-2)) leading, however, to only partial dechlorination (only one chlorine detached from the ring).

$$TiO_2 + h\nu \rightarrow TiO_2(e^-_{CB} + h^+_{VB}) \quad \text{(a)}$$

$$h^+_{VB} + OH^-(H_2O) \rightarrow {}^\bullet OH(+H^+) \times (\text{radical attack on 2, 4-D}) \quad \text{(b)}$$

Oxygen-purged dispersions

$$e^-_{CB} + O_2 \rightarrow O_2^{-\bullet} \quad \text{(major path)} \quad \text{(c-1)}$$

$$e^-_{CB} + \text{2, 4-D} \rightarrow \text{dechlorination} \quad \text{(minor path)} \quad \text{(c-2)}$$

$$O_2{}^{-\bullet} + H^+ \rightarrow HOO^\bullet \quad \text{(attack on 2, 4-D)} \quad \text{(c-3)}$$

Nitrogen-purged dispersions

$$e^-_{CB} + \text{2, 4-D} \rightarrow \text{dechlorination} \quad \text{(major path)} \quad \text{(d)}$$

In the first 15 min of irradiation, the dynamics of Cl^- ion formation varied as $PD_{O_2} \approx PD_{N_2} > PD/MW_{N_2} > PD/MW_{O_2}$, after which it varied as $PD/MW_{O_2} > PD_{O_2} >>> PD_{N_2} \approx PD/MW_{N_2}$. These observations are different from those observed for the formation of Cl^- ions under air-equilibrated conditions. Microwave irradiation has a lesser influence on dechlorination through reaction (d) when the PD/MW_{N_2} route is taken (the residual available oxygen in this case still competes for electrons). In oxygenated dispersions, the degradation of 2,4-D by the PD/MW_{O_2} route is remarkable yielding intermediates, which are fully dechlorinated after only 30 min. We infer that dechlorination ensues after degradation of the 2,4-D structure. Dechlorination is somewhat attenuated by the MW radiation, which explains why formation of Cl^- ions by the PD/MW_{O_2} route is lower than that by the PD_{O_2} route, at least in the first 15 min of irradiation. Evidently, dechlorination of 2,4-D by the PD/MW_{O_2} route is slower initially because the degradative process is mostly focused on converting the carbons in 2,4-D. Under inert conditions (PD/MW_{N_2}), the microwave radiation does not seem to promote reaction (d), and yet degradation is improved by microwave irradiation in the presence of a small quantity of oxygen [34]. However, it is not clear whether degradation is accelerated when no oxygen is present in the dispersions.

The relative ratios of the degradation dynamics of the microwave influence on the photodegradation of 2,4-D, as well as the influence of the atmospheric conditions used (nitrogen or oxygen purging; columns 2 and 3), together with the effect of added oxygen versus nitrogen (columns 4 and 5) are summarized in Table 1. The data show that the microwave radiation does lead to overall greater degradation efficiency, as well as dechlorination of the 2,4-D substrate. Moreover, degradation of 2,4-D was far more efficient in oxygenated dispersions than in nitrogen-purged systems, as evidenced by the decrease of the average UV absorption features at the three wavelengths examined (1.3 times = 1.70/1.35) and by the decrease of total organic carbon (1.6 times = 2.04/1.24). As well, formation of Cl^- ions was faster in oxygenated

Table 1
Relative ratios of the rates of loss of UV absorption, loss of TOC and formation of chloride ions in oxygen- and nitrogen-purged dispersions for the PD and PD/MW routes

	$(PD/MW_{N_2})/(PD_{N_2})$	$(PD/MW_{O_2})/(PD_{O_2})$	$(PD_{O_2})/(PD_{N_2})$	$(PD/MW_{O_2})/(PD/MW_{N_2})$
Uv_{av}	1.35	1.70	1.96	2.51
TOC	1.24	2.04	1.75	2.88
Cl^- ion	1.21	1.64	3.85	2.84

dispersions (1.36 = 1.64/1.21)—compare columns 2 and 3 of Table 1. In the case of the PD/MW route, the greater efficiency of the degradation under oxygenated conditions was confirmed only for the decrease of UV absorption and TOC loss (columns 4 and 5). By contrast, for dechlorination, the efficiency of added oxygen for the PD/MW route was lower than that by the PD route (compare columns 4 and 5). The effect of added oxygen in the PD route alone was expected (column 4). The decrease of UV absorption, the loss of TOC, and the formation of Cl^- ions by the PD/MW_{O_2} route were greater than those by the other methods (see also results depicted in Fig. 5). Note that considerations of the data of Table 1 pertain to show only the relative microwave radiation effect and the effect of added oxygen to the dispersions.

Carboxylic acid intermediates (acetic acid and formic acid) are produced during the degradation of 2,4-D. The relevant data are illustrated in Fig. 6a and b for air-equilibrated conditions; Fig. 6c and d display the effect of the presence of oxygen and nitrogen for the PD and PD/MW routes. Formation of acetic acid was confirmed for the PD/MW and PD/TH routes reaching maximal quantities (ca. 0.15 and ~0.05 mM, respectively) at 15 min of irradiation. However, none formed by the photocatalytic PD route. A small amount of formic acid (maximal after 7 and 22 min of irradiation) was seen for PD, PD/TH and PD/MW under air-equilibrated conditions. The first maximal fraction of formic acid is due to the transformation of the acetic acid function in the 2,4-D structure, whereas the second maximum is likely caused by the conversion of acetic acid initially produced from the degradation of the remaining structure of 2,4-D (compare the data of Fig. 5a and b). For the oxygen- or nitrogen-purged dispersions, the PD_{N_2} and PD/MW_{O_2} routes produced acetic acid after 15 min of irradiation (ca. 0.14 and 0.03 mM, respectively), subsequent to which it degraded further on additional irradiation. Formation of acetic acid was slower by the PD_{O_2} route requiring irradiation of the dispersion for at least 30 min (ca. 0.05 mM; Fig. 6c). By comparison, the PD/MW_{O_2} route produced the largest quantity of formic acid (0.20 mM; Fig. 6d), with the amounts produced by the PD_{O_2}, PD_{N_2}, and PD/MW_{N_2} routes being rather negligible. The peculiar variations in the formation of formic acid and acetic acid through the PD/MW and PD routes under the various atmospheric conditions are noteworthy. Evidently, a synergism exists between microwave irradiation and the nature and quantity of the gases (O_2 versus N_2) present in the dispersions. No doubt, this synergism also affects the mechanistic details of the photodegradative process.

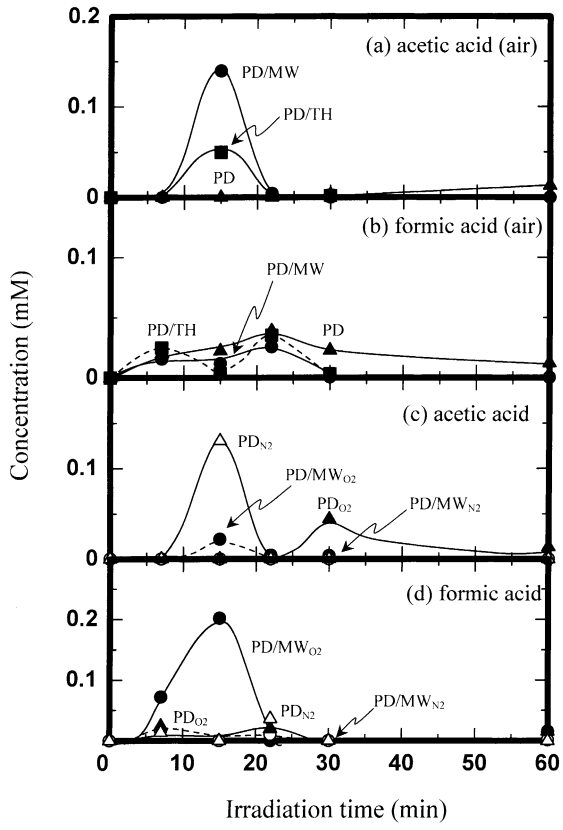

Fig. 6. Temporal evolution of the formation of carboxylic acid intermediates during the degradation of 2,4-D from the methods used in Fig. 5.

3.1. Detection and identification of intermediates

Detection and identification of the intermediates produced during the degradation of the 2,4-D substrate were carried out by electrospray mass spectral techniques. Typical intermediates were identified from both positive (M + H or M + Na) and negative (M − H) modes for the initial substrate, and after 15, 30 and 60 min of irradiation by the PD route and after 15 and 30 min for the PD/MW route under air-equilibrated conditions. The relevant mass spectral data are displayed in Fig. 7. The signals of the initial 2,4-D substrate solution were observed at m/z = 161,163 and 165, and also at m/z = 219, 221, 223 in the negative spectral mode (see Fig. 7 (i-negative))—the three peaks are consistent with a substance having two chlorine substituents with mass ratios of 100:64:10. The main signal at m/z = 219, 221, 223 belongs to the initial 2,4-D toxin as attested to from the database of standards from the LC–MSD manufacturer (Agilent Technologies), whilst the signal at m/z = 161, 163 and 165 is that of dichlorophenol, which was either present as an impurity and/or formed from the degradation of 2,4-D during workup in the electrospray mass spectral detector.

The initial formation of intermediates containing chlorine substituents by the PD and PD/MW routes is shown in Fig. 7 (ii- and v-negative, respectively). The signal at m/z = 235 belongs to intermediate **I** (6-hydroxy-2,4-dichlorophenoxyacetic acid) following irradiation for 15 min. The signals at m/z = 190.9 (**II**), 143 (**V**) and 161 (**III**) in the PD method at 30 min are those of 2,4-dichlorophenoxymethanol, 4-chloro-1,2-benzenediol (i.e. 4-chlorocatechol), and 2,4-dichlorophenol. Signals at m/z = 160.9 (**III**), 177.1 (**IV**) and 190.9 (**II**) were also observed after an irradiation period of 60 min. The signal at m/z = 177.1 is that expected for 3,5-dichloro-1,2-benzenediol (**IV**). Likewise,

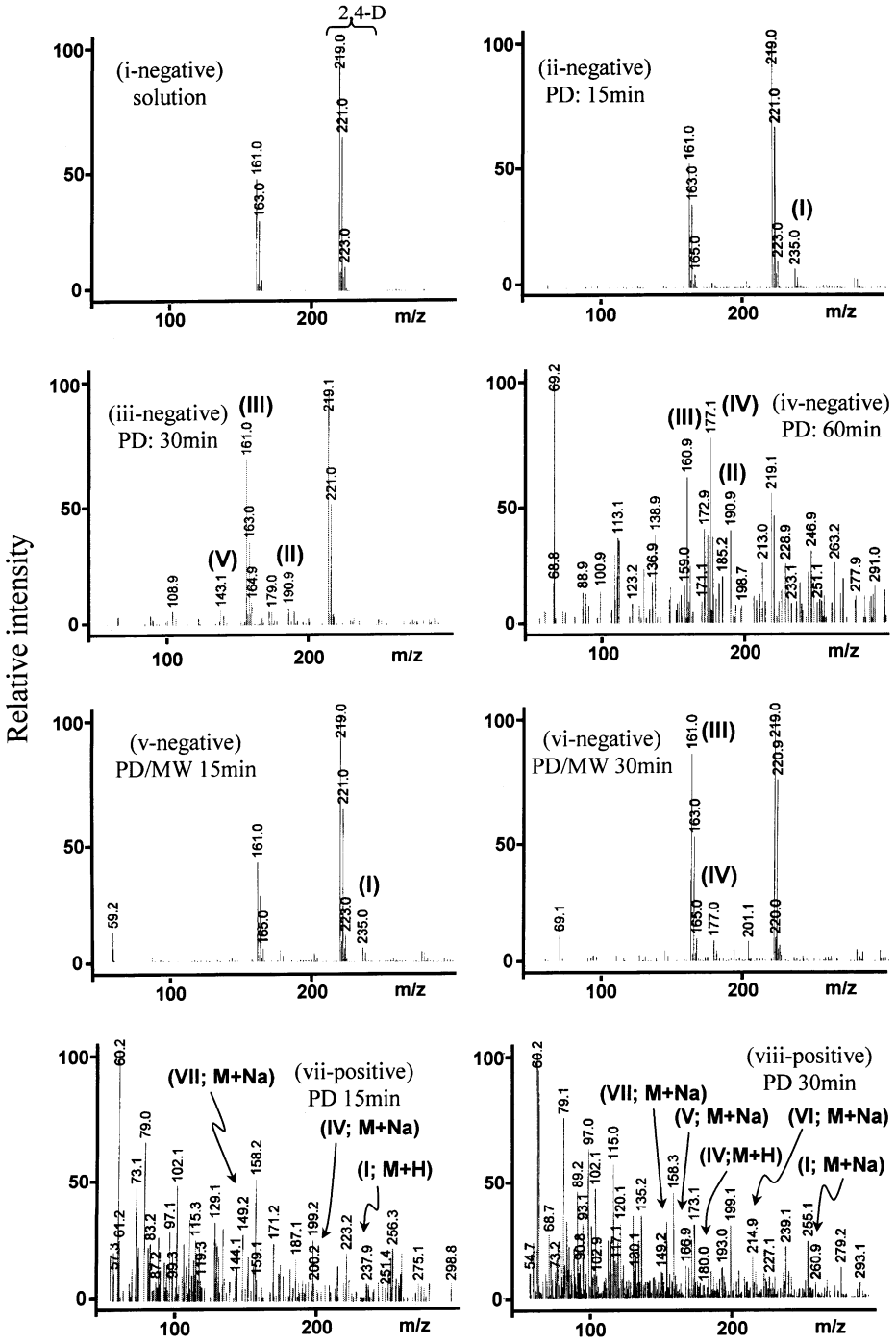

Fig. 7. Electrospray mass spectra in the negative and positive modes recorded during the photodecomposition of 2,4-D by the PD method at 0, 15, 30 and 60 min of irradiation (i–iv-negative), and for the PD/MW method for 15 and 30 min of irradiation (v- and vi-negative). Also shown are the positive mode ESI spectra (vii- and viii-positive) for the PD method after 15 and 30 min of irradiation.

signals at $m/z = 161$ (**III**) and 177 (**IV**) were also observed as significant intermediates for the PD/MW route after a 30 min irradiation period (see Fig. 7 (vi-negative)). The 2,4-dichlorophenoxymethanol signal expected at $m/z = 179$ (**II**) was never seen for the PD/MW method.

Signals in the positive ion mode at $m/z = 149$ (**VII**; M + Na), 166.9 (**V**; M + Na), 180 (**IV**; M + H), 200.2 (**IV**; M + Na), 214.9 (**VI**; M + Na), 237.9 (**I**; M + H) and 260.9 (**I**; M + Na) were observed for the PD route for irradiation times of 15 and 30 min. In particular, the signals at $m/z = 149$ and 214.9 are those of 1,2,4-benzenetriol (**VII**) and 2,4-dichlorophenoxyformaldehyde (**VI**), respectively. Intermediate **III** (viz. 2,4-dichlorophenol) was confirmed on the basis of the mass spectrum of the initial 2,4-D

solution (Fig. 7 (i-negative)). Accordingly, intermediate **III** in Fig. 7 (iii-, iv-, and vi-negative) is that of the intermediate produced from the photodegradation of 2,4-D because the ratio of the peak intensity for $m/z = 161$ and 219 from the 2,4-D solution was initially about 1:2, but was not so in the other mass spectra of Fig. 7.

The above results and discussion suggest the initial mechanistic steps illustrated in Scheme 1 for the photodegradation of 2,4-D by the PD and PD/MW routes under air-equilibrated conditions.

The initial step in the PD route is cleavage of the C–C bond in the $–CH_2{}^{-}COOH$ group in 2,4-D to yield subsequently formic acid and 2,4-dichlorophenoxymethanol (**II**) through addition of a $^{\bullet}OH$ radical to the $–^{\bullet}CH_2$ fragment (step A). Degradation of intermediate (**II**) produces 2,4-dichlorophenoxyformaldehyde (**VI**), which on further irradiation yields 2,4-dichlorophenol (**III**), followed by formation of 3,5-dichloro-1,2-benzenediol (**IV**) and 4-chloro-1,2-benzenediol (i.e. 4-chlorocatechol; **V**). In step B, the 6-hydroxy-2,4-dichlorophenoxyacetic acid (**I**) was formed by attack of $^{\bullet}OH$ radicals on the benzene ring, after which it led to the 3,5-dichloro-1,2-benzenediol species (**IV**) and to 4-chlorocatechol (**V**). For the PD/MW route, degradation of 2,4-D gave initially 6-hydroxy-2,4-dichlorophenoxyacetic acid (**I**) by the same mechanism as the PD route (step C). The acetic acid and formic acid intermediates were preceded by cleavage of the O–C bond in the $O–CH_2COOH$ fragment of 6-hydroxy-2,4-dichlorophenoxyacetic acid (**I**) and of 2,4-D (step D) to give the 2,4-dichlorophenol intermediate (**III**) and subsequently the 3,5-dichloro-1,2-benzenediol species (**IV**). The differences in these initial degradations are due to the initial cleavage position of the 2,4-D molecular structure. In other words, the C–C bond (347 kJ mol^{-1}) fragment was cleaved in the PD route, whereas the O–C bond (352 kJ mol^{-1}) was cleaved in the PD/MW method.

The dependence of the photodegradation of the organic pollutant/TiO_2 dispersion on pH was also examined. The co-aggregation of TiO_2 particles, change of zeta-potential of the TiO_2 surface, and the occurrence of $^{\bullet}OH$ radicals are all affected by the differences in the pH of the aqueous media. The initial pH of the 2,4-D solution was 3.8, which on addition of TiO_2 particles rose to ca. pH 4. After this very small change in pH, no other significant pH changes were observed following irradiation by MW and/or UV light for each of the routes examined under our experimental conditions.

3.2. Photodegradation of 2,4-D with the DQCPP reactor

The decrease of UV absorption features at 229 nm, loss of TOC, and formation of Cl^{-} ions during the photodegradation of 2,4-D in the DQCPP reactor are illustrated in Fig. 8 for irradiation times of 10, 20 and 30 min. The advantage of the DQCPP reactor rests on the following considerations: (a) the microwaves provide the energy source for the UV light and microwave radiation so that the device is greatly simplified; (b) degradation of 2,4-D by the PD/MW route is expected because all of the microwave power is not completely changed into UV light; and (c) the efficiency of light

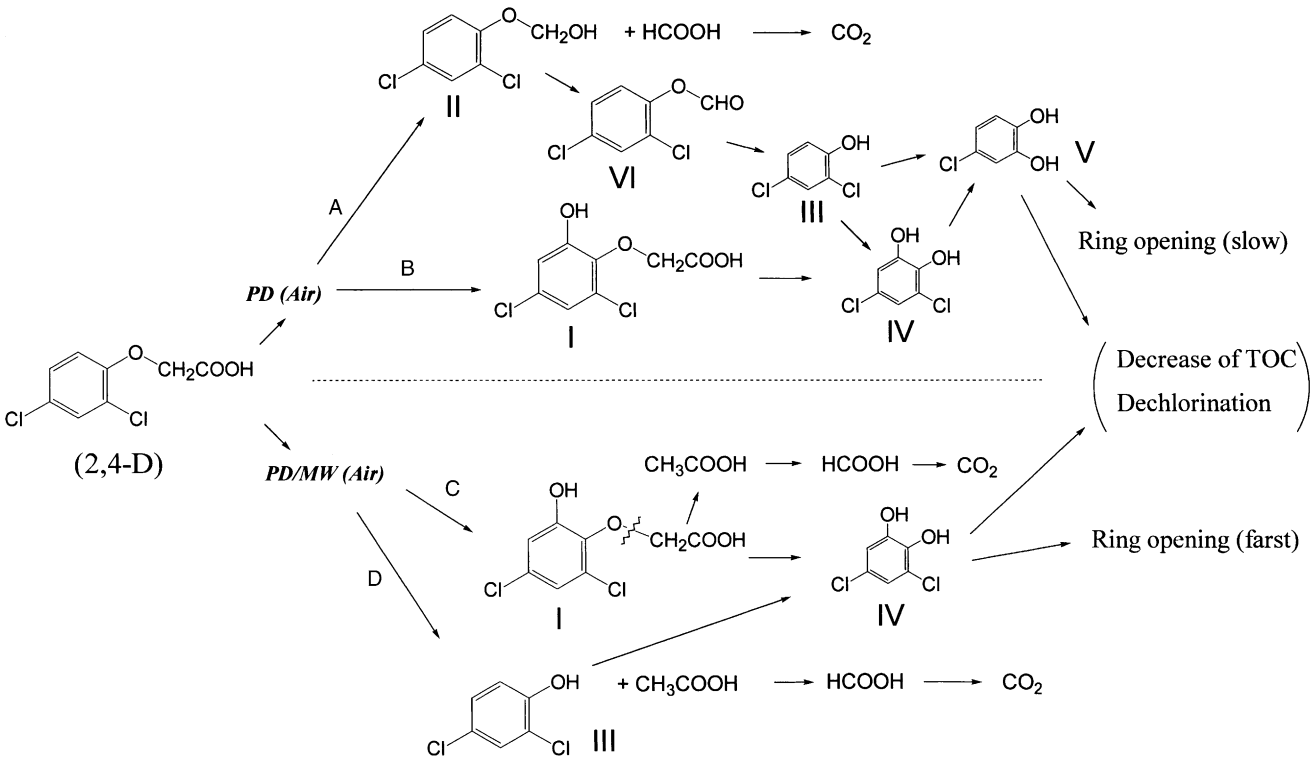

Scheme 1. Proposed initial degradation mechanism of the photodegradation of 2,4-D by the PD and PD/MW methods under air-equilibrated conditions.

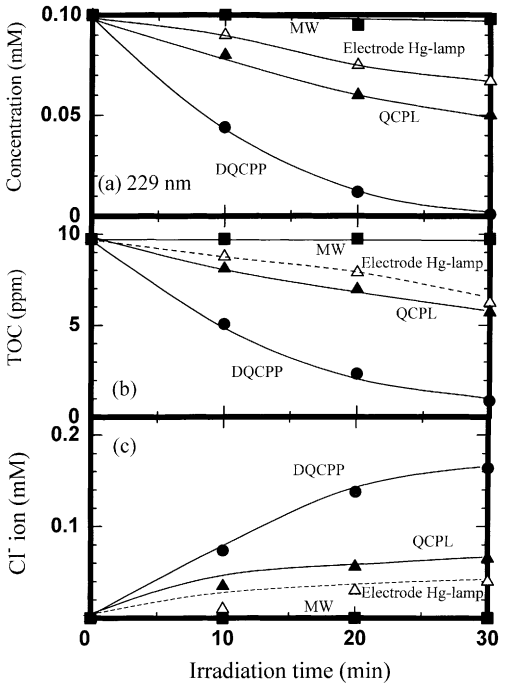

Fig. 8. Disappearance of 2,4-D as evidenced by loss of UV absorption at 229 nm, loss of TOC and formation of Cl^- ions during the degradation of 2,4-D in aqueous 1,4-D/TiO_2 dispersions irradiated using the DQCPP device, microwave radiation, UV light from the electrode Hg lamp, and UV light from the electrodeless Hg lamp system for irradiation times of 15, 30 and 60 min.

irradiation with the DQCPP lamp system is greater than that with the electrode Hg lamp. Microwave irradiation alone without the DQCPP device had no effect on the 2,4-D toxin.

No UV absorption feature at 229 nm was observed after only 30 min of irradiation of the 2,4-D/TiO_2 dispersion, indicating complete degradation of the 2,4-D substrate when using the DQCPP system (Fig. 8a). In the case of the PD route, which used the electrode Hg lamps, and the PD/MW route, which used the electrodeless Hg lamps (QCPL), the extent of degradation of 2,4-D was 33 and 50%, respectively, achieved under otherwise identical conditions. The mineralization of the 2,4-D solution was also assessed by TOC assays (Fig. 8b). The corresponding loss of the initial TOC (10 ppm) was about 91, 20 and 33% when using, respectively, the DQCPP reactor, the electrode Hg lamp, and the QCPL for a 30 min irradiation period. The corresponding degree of dechlorination (Fig. 8c) of 2,4-D was 82, 60 and 55%, respectively. Note again that microwave irradiation alone had no effect on the photodegradation of 2,4-D. The above characteristics of the decomposition of 2,4-D are the same as those observed in the batch system (see Fig. 3).

The electric power used to power the electrode and electrodeless Hg lamp systems was in both cases 150 W. However, the average light irradiance for the electrode Hg lamp was three times greater (12 mW cm^{-2}) than that of the electrodeless lamp (4 mW cm^{-2}). Clearly, the photodegradation of 2,4-D by the PD/MW route (air), even at the smaller light irradiance of 4 mW cm^{-2}, was faster than by the PD route at the higher light irradiance of 12 mW cm^{-2}. Evidently, microwave radiation enhances the overall degradation and makes up for the poor transparency of the dispersion and the lower irradiance used.

Acknowledgements

We are grateful to the Japanese Ministry of Education, Culture, Sports, Science and Technology for a Grant-in-aid for Scientific Research (no. 10640569 to HH), and to the Natural Sciences and Engineering Research Council of Canada (no. A5443 to NS) for support of our work. We are also grateful to N. Watanabe, A. Tokunaga and A. Saitou for expert technical assistance.

References

[1] E. Pellizzetti, V. Maurino, C. Minero, V. Carlin, E. Pramauro, O. Zerbinati, M.L. Tosato, Environ. Sci. Technol. 24 (1990) 1559.
[2] P.L. Yue, D.P. Allen, in: D.F. Ollis, H. Al-Ekabi (Eds.), Photocatalytic Purification and Treatment of Water and Air, Elsevier, Amsterdam, 1993, p. 607.
[3] I. Texier, J. Ouazzani, J. Delaire, C. Giannotti, Tetrahedron 55 (1999) 3401.
[4] E. Pelizzetti, C. Minero, P. Piccinini, M. Vincenti, Coord. Chem. Rev. 125 (1993) 183.
[5] E. Chamarro, S. Esplugas, J. Chem. Technol. Biotechnol. 57 (1993) 273.
[6] P. Pichat, J.C. D'Oliveira, J.F. Maffre, D. Mas, in: D.F. Ollis, H. Al-Ekabi (Eds.), Photocatalytic Purification and Treatment of Water and Air, Elsevier, Amsterdam, 1993, p. 683.
[7] T.S. Muller, Z. Sun, G. Kumer, K. Itoh, M. Murabayashi, Chemosphere 36 (1998) 2043.
[8] A.D. Modestov, O. Lev, J. Photochem. Photobiol. A: Chem. 112 (1998) 261.
[9] T. Naguyen, D.F. Ollis, J. Phys. Chem. 88 (1984) 3386.
[10] D.W. Bahnemann, J. Moning, R. Chapman, J. Phys. Chem. 91 (1987) 3782.
[11] M. Barbeni, M. Morello, E. Pramauro, E. Pelizzetti, M. Vincenti, E. Borgarello, N. Serpone, M.A. Jamieson, Chemosphere 16 (1987) 1165.
[12] F. Sabin, T. Turk, A. Vogler, J. Photochem. Photobiol. A: Chem. 63 (1992) 99.
[13] R. Borello, C. Minero, E. Pramauro, E. Pelizzetti, N. Serpone, H. Hidaka, Environ. Toxicol. Chem. 8 (1989) 997.
[14] E. Pelizzetti, M. Barbeni, E. Pramauro, N. Serpone, E. Borgarello, M.A. Jamieson, H. Hidaka, Chim. Ind. (Milano) 67 (1985) 623.
[15] H. Al-Ekabi, N. Serpone, J. Phys. Chem. 92 (1988) 5726.
[16] J.-C. D'Oliveira, G. Al-Sayyed, P. Pichat, Environ. Sci. Technol. 24 (1990) 990.
[17] W. Lee, Y.-M. Gao, K. Dwight, A. Wold, Mater. Res. Bull. 27 (1992) 685.
[18] Y. Ku, C.B. Hsieh, Water Res. 26 (1992) 1451.
[19] J.-C. D'Oliveira, C. Minero, E. Pelizzetti, P. Pichat, J. Photochem. Photobiol. A: Chem. 72 (1993) 261.
[20] F. Nome, A.F. Rubira, C. Franco, L.G. Ionescu, J. Phys. Chem. 86 (1982) 1881.
[21] J.H. Carey, J. Lawrence, H.M. Tosine, Bull. Environ. Contain. Toxicol. 16 (1976) 697.
[22] E. Pelizzetti, M. Borgarello, C. Minero, E. Pramauro, E. Borgarello, N. Serpone, Chemosphere 17 (1988) 499.

[23] P. Zhang, R.J. Scrudato, J.J. Pagano, R.N. Roberts, in: D.F. Ollis, H. Al-Ekabi (Eds.), Photocatalytic Purification and Treatment of Water and Air, Elsevier, Amsterdam, 1993, p. 619.
[24] S. Tunesi, M.A. Anderson, Chemosphere 16 (1987) 1447.
[25] E. Pelizzetti, V. Carlin, C. Minero, M. Gratzel, New J. Chem. 15 (1991) 351.
[26] E. Pelizzetti, V. Maurino, C. Minero, V. Carlin, E. Pramauro, O. Zerbinati, M.L. Tosata, Environ. Sci. Technol. 24 (1990) 1559.
[27] M. Barbeni, E. Pramauro, E. Pelizzetti, E. Borgarello, N. Serpone, M.A. Jamieson, Chemosphere 15 (1986) 1913.
[28] M. Barbeni, E. Pramauro, E. Pelizzetti, Chemosphere 14 (1985) 195.
[29] G. Li Puma, P.L. Yue, in: D.F. Ollis, H. Al-Ekabi (Eds.), Photocatalytic Purification and Treatment of Water and Air, Elsevier, Amsterdam, 1993, p. 689.
[30] C. Minero, E. Pelizzetti, S. Malato, J. Blanco, Chemosphere 26 (1993) 2103.
[31] V.B. Manilal, A. Haridas, R. Alexander, G.D. Surender, Water Res. 26 (1992) 1035.
[32] G. Mailhot, M. Astruc, M. Bolte, Appl. Organometal. Chem. 13 (1999) 53.
[33] K. Harada, K. Tanaka, T. Hisanaga, S. Murata, Mizusyorigijyutu 26 (1985) 917.
[34] S. Horikoshi, H. Hidaka, N. Serpone, Environ. Sci. Technol. 36 (2002) 1357.
[35] S. Horikoshi, H. Hidaka, J. Jpn. Soc. Color Mater. 75 (2002) 180.
[36] S. Horikoshi, H. Hidaka, Chem. Ind. 53 (2002) 740.
[37] S. Horikoshi, H. Hidaka, N. Serpone, Environ. Sci. Technol. 36 (2002) 5229.
[38] S. Horikoshi, H. Hidaka, N. Serpone, J. Photochem. Photobiol. A: Chem. 53 (2002) 183.
[39] S. Horikoshi, N. Serpone, S. Yoshizawa, J. Knowland, H. Hidaka, J. Photochem. Photobiol. A: Chem. 120 (1999) 63.
[40] (a) H.M. Kingston, S.J. Haswell (Eds.), Microwave-Enhanced Chemistry, American Chemical Society, Washington, DC, 1997;
(b) A. Loupy (Ed.), Microwaves in Organic Synthesis, Wiley-VCH Verlag, Weinheim, Germany, 2002.
[41] (a) D. Stuerga, M. Delmotte, in: A. Loupy (Ed.), Microwaves in Organic Synthesis, Wiley-VCH Verlag, Weinheim, Germany, Chapter 1, p. 17, 2003;
(b) D.R. Baghurst, D. Michael, P. Mingos, in: H.M. Kingston, S.J. Haswell (Eds.), Microwave-Enhanced Chemistry, American Chemical Society, Washington, DC, Chapter 10, p. 532, 1997.
[42] (a) A.V. Emeline, G.N. Kuzmin, D. Purevdorj, V.K. Ryabchuk, N. Serpone, J. Phys. Chem. B 104 (2000) 2989;
(b) A.V. Emeline, G.V. Kataeva, V.K. Ryabchuk, N. Serpone, J. Phys. Chem. 103 (1999) 9190;
(c) A.V. Emeline, E.V. Lobyntseva, V.K. Ryabchuck, N. Serpone, J. Phys. Chem. 103 (1999) 1325;
(d) A.V. Emeline, S.V. Petrova, V.K. Ryabchuck, N. Serpone, Chem. Mater. 10 (1998) 3484;
(e) A.V. Emeline, G.V. Kataeva, A.S. Litke, A.F. Rudakova, V.K. Ryabchuck, N. Serpone, Langmuir 14 (1998) 5011.
[43] S. Horikoshi, H. Hidaka, N. Serpone, Environ. Sci. Technol. 36 (2002) 1357.
[44] J.H. Booske, R.F. Cooper, I. Dobson, J. Mater. Res. 7 (1992) 495.
[45] A.V. Emeline, A.V. Frolov, V.K. Ryabchuk, N. Serpone, J. Phys. Chem. B, submitted for publication.